

Quark Nugget Dark Matter: Comparison with radio observations of nearby galaxies.

K. Lawson and A.R. Zhitnitsky

Department of Physics & Astronomy, University of British Columbia, Vancouver, B.C. V6T 1Z1, Canada

It has been recently claimed that radio observations of nearby spiral galaxies essentially rule out a dark matter source for the galactic haze[1]. Here we consider the low energy thermal emission from a quark nugget dark matter model in the context of microwave emission from the galactic centre and radio observations of nearby Milky Way like galaxies. We demonstrate that observed emission levels do not strongly constrain this specific dark matter candidate across a broad range of the allowed parameter space in drastic contrast with conventional dark matter models based on the WIMP paradigm.

I. INTRODUCTION

The galactic microwave ‘haze’ was first detected in the WMAP data [2] and was subsequently confirmed by Planck [3]. This haze is characterized as diffuse continuum emission, centred on the galactic centre and with a harder spectrum than expected for galactic synchrotron emission. It is generally believed to be due to the synchrotron emission from the injection of a distinct population of high energy particles within the galactic centre which are subsequently deflected by the galactic magnetic field. The source of these high energy particles has been speculated to be either a recent outburst from the galactic centre or possibly the decay or annihilation of dark matter particles into relativistic standard model particles.

The main motivation for the present work is the claim [1] that radio observations of nearby spiral galaxies essentially rule out a dark matter source for the galactic haze. This claim is based on the assumption that if the haze is produced by dark matter annihilation or decay, this emission must continue with a similar spectral index down to radio frequencies. If this is the case then similar diffuse radio halos should exist around other galaxies provided they have a similar distribution of matter and dark matter. It is important that all conventional dark matter models based on the weakly interacting massive particle (WIMP) paradigm do indeed predict a synchrotron spectrum which continues from microwave frequencies with $\nu \geq 22$ GHz to radio frequencies with $\nu \leq 1$ GHz. Therefore, the assumptions of [1] on the continuity of the spectrum are well justified for WIMP based models.

Here we study the same question of radio emission from spiral galaxies but in a drastically different model, one in which the dark matter is represented by macroscopically large nuggets of standard model quarks, similar to the Witten’s strangelets [4], see section III for a short overview of this model. In this model the haze signal is generated by the thermal emission from a population of macroscopically large nuggets which may constitute the galactic dark matter. While this thermal spectrum is similar to the observed haze spectrum across the microwave band it falls rapidly at lower frequencies due to many body effects, as we shall argue below. Consequently, the constraints imposed by radio band emission

from nearby galaxies is considerably weaker than in the case of conventional WIMP type (decaying or annihilating) dark matter models. This claim represents the main result of the present work.

Following a brief review of the properties of the galactic haze (section II) we provide an overview of the quark nugget dark matter model in section III. With these basics in place we layout the process by which the nuggets may give rise to a component of the observed haze emission in section IV and compare the predicted spectrum to radio band observations in section V. Our conclusions are presented in section VI.

II. THE GALACTIC HAZE

Initial observations of the haze indicated that it should be considered a unique component of the galactic spectrum with a spectral index softer than that of free-free emission and harder than that expected for galactic synchrotron. Current estimates based on Planck data give a spectral index of $\beta_H = -2.55 \pm 0.05$ such that $T_\nu \sim \nu^{\beta_H}$ [3]. In addition to the differing spectral index a free-free emission interpretation of the haze is disfavoured by the lack of correlated $H\alpha$ emission. Morphologically the haze is found to be centred on the galactic centre extending over galactic longitudes $|l| < 15^\circ$ and galactic latitudes $|b| < 35^\circ$ with an approximately $1/r$ fall off in intensity across that range.

If the haze is generated by synchrotron emission from a population of relativistic particles then there should be a correlated diffuse γ -ray emission arising from the inverse Compton scattering of these particles. Such a component has been detected by the Fermi Gamma-Ray Space Telescope [5]. Subsequent observations have demonstrated that the γ -ray component displays relatively sharp edges at high latitudes, these features are now referred to as the Fermi bubbles [6]. Planck also detects a polarized component of the haze which is well correlated with both the observed morphology and spectrum of the unpolarized observations [7]. This combination of features seems to support the idea that the haze is generated by the injection of a population of high energy electrons strongly correlated with the galactic centre. However, the source of such a population of relativistic particles remains un-

known. A variety of sources have been suggested, but they seem to have difficulty describing all aspects of the observed emission. In particular the combination of a very sharp edge at large latitudes and strong intensity at low latitudes is difficult to reproduce [8]. The sharp edges of the bubbles are a noted feature in both the microwave and γ -ray morphology and strongly favour a transient high energy event associated with astrophysical processes in the galactic centre. Conversely, the absence of limb darkening at low latitudes favours a process involving the continuous injection of the required population of high energy particles. It has been suggested that dark matter annihilations or decays may be responsible for injecting these particles. However, this interpretation is disfavoured by the sharp bubble edges at large latitudes which do not naturally appear in cosmic ray propagation models involving a continuous injection of particles.

The difficulty in reproducing the morphology of the haze with either a transient event in the galactic centre or dark matter emission has also lead to the consideration of hybrid models in which only a fraction of the haze intensity is provided by dark matter. The analysis of [9] found that the fit to observations is substantially improved if the Fermi bubble correlated emission is supported by an additional dark matter contribution at the $\approx 20\%$ level. However, without a well established mechanism for the generation of the Fermi bubbles and associated microwave emission any component separation remains subject to large uncertainties.

If the haze is in fact supported by dark matter annihilations or decays then one should expect similar emission to be associated with the dark matter halos of nearby galaxies. Conversely, if the haze is the result of a transient event in the galactic centre there is no reason to expect to detect haze like emission from other galaxies. As the haze emission generated by relativistic particles injected into the galactic centre will be continuous between the microwave and radio bands radio observations of nearby galaxies can be used to differentiate between these two models as argued in [1]. An analysis of nearby spiral galaxies shows that they underproduce radio band haze relative to the milky way disavouring the conventional dark matter interpretation of the haze signal [1].

With this background in place we will study the same question but in a drastically different dark matter model which does contribute to the galactic haze but at the same time is not subject to constraints coming from radio band emission, similar to studies of ref.[1].

III. QUARK NUGGET DARK MATTER

In this section we will give a brief overview of the quark nugget dark matter model. For further details see the original papers [10–12] as well as the recent short review [13].

The idea that the dark matter may take the form of composite objects composed of standard model quarks in

novel phase goes back to stranglet models [4]. In these models the presence of strange quarks stabilizes quark matter at sufficiently high densities, allowing strangelets formed in the early universe to remain stable over cosmological timescales. The quark nugget model is conceptually similar, with the nuggets being composed of a stable high density colour superconducting phase. The only new crucial element proposed in [10, 11], in comparison with the earlier studies of [4] is that the nuggets can be made of antimatter as well as matter in this framework.

The original motivation for this model was unrelated to explaining any particular galactic emission source but was related to the seemingly unrelated problem of the nature of baryogenesis. It is generally assumed that the universe began in a symmetric state with zero global baryonic charge and later (through some baryon number violating process) evolved into a state with a net positive baryon number as observed today. As an alternative to this scenario we advocate a model in which “baryogenesis” is actually a charge separation process in which the global baryon number of the universe remains zero. In this model the unobserved antibaryons come to comprise the dark matter in form of dense quark (anti) nuggets. A connection between dark matter and baryogenesis is made particularly compelling by the similar energy densities of the visible and dark matter with $\Omega_{\text{dark}} \simeq 5 \cdot \Omega_{\text{visible}}$. If these processes are not fundamentally related the two components could easily exist at vastly different scales.

The observed matter to dark matter ratio corresponds to a scenario in which the number of antinuggets is larger than number of nuggets by a factor of $\sim 3/2$ at the end of the nuggets’ formation at the QCD temperature $T_{\text{form}} \sim \Lambda_{\text{QCD}}$ when conventional baryonic visible matter forms. This would result in a matter content with baryons, quark nuggets and antiquark nuggets in an approximate ratio

$$B_{\text{visible}} : B_{\text{nuggets}} : B_{\text{antinuggets}} \simeq 1 : 2 : 3, \quad (1)$$

with no net baryonic charge.

Unlike conventional dark matter candidates, such as WIMPs the dark-matter/antimatter nuggets are strongly interacting but macroscopically large. They do not contradict any of the many known observational constraints on dark matter or antimatter for three main reasons [12]:

- They carry a huge (anti)baryon charge $|B| \gtrsim 10^{25}$, and so have an extremely tiny number density;
- The nuggets have nuclear densities, so their effective interaction is small $\sigma/M \sim 10^{-10} \text{ cm}^2/\text{g}$, well below the typical astrophysical and cosmological limits which are on the order of $\sigma/M < 1 \text{ cm}^2/\text{g}$;
- They have a large binding energy such that baryon charge in the nuggets is not available to participate in big bang nucleosynthesis (BBN) at $T \approx 1 \text{ MeV}$.

To reiterate: the weakness of the visible-dark matter interaction is achieved in this model due to the small geometrical parameter $\sigma/M \sim B^{-1/3}$ rather than due to

a weak coupling of a new fundamental field with standard model particles. In other words, this small effective interaction $\sim \sigma/M \sim B^{-1/3}$ replaces a conventional requirement of sufficiently weak interactions of the visible matter with WIMPs.

A. Nugget properties

The nuggets consist of light standard model quarks bound into a colour superconducting state in which the quarks form cooper pairs analogous to those found in a traditional superconductor. The exact pairing structure, and thus the behaviour of the low energy excitations of the quark matter are dependent on the details of the high density QCD phase diagram, which remains an open research topic, see for example the review [14]. At large densities the pairing of quarks with unique quantum numbers favours the presence of equal numbers of u, d and s quarks. However, the relatively large mass of the strange quarks causes their relative depletion at lower densities. This results in a net charge for the quark nugget (positive in the case of quarks and negative in the case of antiquarks) which is compensated for by a layer of leptons known as the ‘electrosphere’ which surrounds the nugget. The majority of the observational properties of the nuggets are dictated by the properties of the electrosphere, as discussed below, and consequently, are not strongly sensitive to the exact details of the quark matter. In particular the low energy thermal emissions that are the primary concern of this work are produced in the outer layer of the electrosphere, known as the “Boltzmann” regime, where the positron density has dropped sufficiently to become transparent to low energy photons.

Physically the nuggets will be macroscopically large with a combination of theoretical and observational constraints suggesting an average nugget baryon number in the range $10^{25} < B < 10^{33}$. Assuming typical nuclear scale densities this translates to an average radius in the range $10^{-5}\text{cm} < R_N < 10^{-3}\text{cm}$, and to a mass in the range from 1g up to thousands of tons. As stated above, the most important physical property in terms of scaling the observational consequences of a dark matter model is the cross-section to mass ratio. Using standard values for the density of quark matter we may estimate,

$$\frac{\sigma}{M} \approx 10^{-10} \frac{\text{cm}^2}{\text{g}} \left(\frac{10^{25}}{B} \right)^{1/3}. \quad (2)$$

B. Present constraints

While the observable consequences of this model are on average strongly suppressed by the low number density of the quark nuggets the interaction of these objects with the visible matter of the galaxy will necessarily produce observable effects. Any such consequences will be largest where the densities of both visible and dark matter are

largest such as the core of the galaxy or the early universe. In other words, the nuggets behave as conventional cold dark matter in the environment where the visible matter density is small, while they become interacting and emitting radiation objects (i.e. effectively become visible matter) when in an environment with sufficiently large density.

The features of the nuggets relevant for phenomenology are determined by the properties of the electrosphere, as we have already mentioned. The relevant computations can be found in original refs. [15–21]. These properties are in principle, calculable from first principles using only the well established and known features of QCD and QED. As such the model contains no tunable fundamental parameters, except for a single mean baryon number of the nuggets $\langle B \rangle$.

There are currently a number of both ground based and astrophysical observations which impose constraints on allowed quark nugget dark matter parameters. These include the non-detection of a nugget flux by the IceCube monopole search [22] which limits the flux of nuggets to $\Phi_N < 1\text{km}^{-2} \text{yr}^{-1}$. Similar limits are likely also obtainable from the results of the Antarctic Impulse Transient Antenna (ANITA) [23] and it has been suggested that large scale cosmic ray detectors may be capable of improving these limits [24]. While ground based direct searches offer the most unambiguous channel for the detection of quark nuggets the flux of nuggets is inversely proportional to the nugget mass and consequently even the largest available detectors are incapable of excluding a nugget flux across their entire potential mass range.

It has also been suggested that the quark nuggets, through their interactions with visible matter, may contribute to astrophysical sources of diffuse emission. Analysis of the nugget emission spectrum and its consequences in a range of galactic and cosmological environments may provide indirect search channels strongly complementary to the direct detection searches outlined above. This type of analysis has been at least partially carried out for several important components of the nugget emission spectrum. For example, the annihilation of the positrons of the electrosphere with incident electrons will contribute to the well known galactic 511 keV line [15]. The positrons farthest from the nugget, with which incoming electrons will dominantly annihilate, carry relatively low momenta making the annihilation spectrum consistent with the narrow 511 keV line observed [16]. As a consequence of the wide range of energy scales involved in the electrosphere the 511 keV line will necessarily be accompanied by a higher energy ($\sim 10 \text{ MeV}$) continuum [17]. While less observational data is available in this range than at either higher or lower energies and the astrophysical backgrounds are large there is a strong indication of a diffuse galactic excess in the MeV range [25]. A detailed analysis of relative annihilation rates suggests that this MeV signal occurs at a level consistent with coproduction with the galactic 511 keV line [19]. At present the uncertainty in the contribution

of conventional astrophysical processes to the 511 keV line make precise constraints on the quark nugget mass difficult to determine. A rough estimate indicates that a population of nuggets with $B \sim 10^{24}$ would saturate the observed 511 keV emission favouring a mean baryon number above this scale.

The annihilation of galactic protons is a more difficult process to study than the relatively simple case of electron-positron annihilations. The majority of the released energy is thermalized and emitted as low energy radiation to be described in detail below. Even in the case of proton annihilations occurring very near the quark surface the energy released will rapidly transfer to the many light positrons generating a local hot spot on the nugget. This process was analyzed in [20] where an x-ray band emission signal was predicted. Uncertainty in the background astrophysics producing the diffuse x-ray spectrum of galactic centre make predictions of a total nugget contribution across this range difficult to estimate. However, there appears to be a hot component to the diffuse x-ray continuum which exceeds known astrophysical energy input [26]. The analysis of [20] demonstrated the consistency of the proposal that the this additional x-ray emission may be coproduced with the galactic 511 keV line. As such, while it provides an important consistency check on the quark nugget dark matter model it does not significantly improve on the limits obtainable from the 511 keV emission strength.

It has been also suggested recently [27] that the interactions of antinuggets with normal matter in the Earth and Sun will lead to annihilation and an associated neutrino flux. Furthermore, it has been claimed [27] that the antiquark nuggets in the interesting region $10^{25} < B < 10^{33}$ cannot account for more than 20% of the dark matter flux based on constraints for the neutrino flux in 20-50 MeV range where the sensitivity of the underground neutrino detectors such as SuperK have their highest signal-to-noise ratio. However, this claim is based on the assumption that the annihilation of visible baryons within an antiquark nugget generates a neutrino spectrum similar to the conventional baryon- antibaryon annihilation spectrum. In a standard baryon- antibaryon annihilation the large number of produced pions eventually decay to muons and consequently to highly energetic neutrinos in the 10-50 MeV energy range. The analysis of [27] assumed that the neutrino spectrum from the annihilation of an antiquark nugget will fall in this same range. However, this spectrum may be very different for annihilations occurring within the colour superconducting nuggets. Within most colour superconducting phases the lightest pseudo Goldstone mesons (the pions and Kaons) have masses in the 5-20 MeV range [14] considerably lighter than in the hadronic confined phase where $m_\pi \sim 140$ MeV. Therefore, these light pseudo Goldstone mesons in the colour superconducting phase¹

will not generally produce highly energetic neutrinos in the 20-50 MeV energy range and thus are not subject to the SuperK constraints employed in [27].

IV. THERMAL EMISSION

We will now use this basic picture of the quark nuggets and their interactions with the surrounding visible matter of the galaxy to extract some basic observational consequences of this model in the radio and microwave bands relevant to the haze. This will involve an analysis of thermal emission from the electrosphere.

A. Electrosphere

As discussed in section III A thermal emission from the nuggets is dominated by the emission of low energy photons from the Boltzmann regime of the electrosphere. Consequently our analysis of this emission will require a brief overview of the properties of this region, here we essentially follow the results of [18, 19].

The mean-field approximation for the positron distribution involves solving the Poisson equation

$$\nabla^2 \phi(\vec{r}) = -4\pi en(\vec{r}) \quad (3)$$

where $\phi(\vec{r})$ is the electrostatic potential and $n(\vec{r})$ is the density of positrons. As the nuggets are larger than the characteristic scale of the electrosphere we are able to work in the one-dimensional approximation

$$\frac{d^2 \phi(z)}{dz^2} = -4\pi en(z) \quad (4)$$

where z is the distance from the quark nugget surface. We now introduce the positron chemical potential $\mu_{e^+}(z) = -e\phi(z)$ which is the potential energy of a charge at position z relative to $z = \infty$ where we take $\mu_{e^+}(\infty) = 0$ as a boundary condition. The Poisson equation (equation 4) may then be formulated in terms of the chemical potential giving

$$\frac{d^2 \mu_{e^+}(z)}{dz^2} = 4\pi \alpha n[\mu_{e^+}(z)] \quad (5)$$

with the additional boundary conditions $\mu_{e^+}(z=0) = \mu_0 \sim 10$ MeV as established by beta-equilibrium in the quark matter. The full density profile, from the quark surface to vacuum, was computed in [19]. However, for our analysis it is only necessary to consider the low density non relativistic Boltzmann regime where

¹ We refer to Appendix 2 of ref.[20] where it has been explicitly

stated that a typical result of the annihilation of visible matter with an anti-nugget is the production of very light $m \sim 10$ MeV mesons which consequently decay to electrons and neutrinos.

$n \ll (mT)^{3/2}$. In this case the positron density is well approximated by

$$n[\tilde{\mu}] \approx 2 \int \frac{d^3 p}{(2\pi)^3} e^{\frac{[\tilde{\mu} - p^2/(2m)]}{T}} = \sqrt{2} \left(\frac{mT}{\pi} \right)^{3/2} e^{\frac{\tilde{\mu}}{T}}. \quad (6)$$

The effective chemical potential $\tilde{\mu} = \mu_{e^+} - m$ is related to the vacuum chemical potential μ by subtracting the mass. We note that the right boundary condition must now be changed to $n(z = \infty) = 0$ because $\tilde{\mu}$ does not tend to zero under these approximations. The left boundary condition must be determined by matching the density at some point to the full relativistic solution that integrates to the quark-matter core. The differential equation (5) has the peculiar solution

$$n(z) = \frac{T}{2\pi\alpha} \frac{1}{(z + \bar{z})^2}, \quad (7)$$

where \bar{z} is an integration constant fixed by matching to a full solution. A proper computation of \bar{z} would require tracking the density through many orders of magnitude from the ultrarelativistic down to the nonrelativistic regime. These computations as we already mentioned, have been carried out in [19]. However, a simple approximation will suffice for present purposes. We take $z = 0$ to define the onset of the Boltzmann regime:

$$n(z = 0) = \frac{T}{2\pi\alpha\bar{z}^2} = (mT)^{3/2}, \quad \frac{1}{\bar{z}} \simeq \sqrt{2\pi\alpha} \cdot m \cdot \sqrt[4]{\frac{T}{m}}. \quad (8)$$

Numerically, $\bar{z} \sim 0.5 \cdot 10^{-8}$ cm while the density $n \sim 0.3 \cdot 10^{23}$ cm $^{-3}$ for $T \simeq 1$ eV. A comparison with the exact numerical results of [19] support our approximate treatment of the problem in terms of parameters represented by equations (7) and (8). In this formulation the region described by $z < 0$ corresponds to the high density regime where the Boltzmann approximation breaks down and which is opaque to thermal photons [19].

B. Thermal spectrum and LPM suppression

In order to determine the thermal spectrum we begin estimating the emissivity of the positrons of the Boltzmann regime, this calculation follows the results of [18] but will provide a more careful treatment of the low energy behaviour than was required in that analysis.

The starting point is the following expression for the cross section for two positrons emitting a soft photon with $\omega \ll p^2/(2m)$, see [18] for the detail discussions on validity of this classical formula,

$$d\sigma_\omega = \frac{4}{15} \alpha \left(\frac{\alpha}{m} \right)^2 \cdot \left(17 + 12 \ln \frac{p^2}{m\omega} \right) \frac{d\omega}{\omega}. \quad (9)$$

The emissivity $Q = dE/dt/dV$ —defined as the total energy emitted per unit volume, per unit time—and the

spectral properties can be calculated from

$$\begin{aligned} \frac{dQ}{d\omega}(\omega, z) &= n_1(z, T) n_2(z, T) \omega \left\langle v_{12} \frac{d\sigma_\omega}{d\omega} \right\rangle \\ &= \frac{4\alpha}{15} \left(\frac{\alpha}{m} \right)^2 n^2(z, T) \left\langle v_{12} \left(17 + 12 \ln \frac{p_{12}^2}{m\omega} \right) \right\rangle \end{aligned} \quad (10)$$

where $n(z, T)$ is the local density at distance z from the nugget's surface, and $v_{12} = |\vec{v}_1 - \vec{v}_2|$ is the relative velocity. The velocity and momentum p_{12} need to be thermally averaged. Assuming the Boltzmann distribution (6) the corresponding computations lead to the following expression [18]:

$$\begin{aligned} \left\langle v_{12} \left(17 + 12 \ln \frac{mv_{12}^2}{\omega} \right) \right\rangle &= \\ &= 2 \sqrt{\frac{2T}{m\pi}} \left(1 + \frac{\omega}{T} \right) e^{-\omega/T} h\left(\frac{\omega}{T}\right) \end{aligned} \quad (11)$$

where the function $h(x)$ for all x can be approximated as follows

$$h(x) = \begin{cases} 17 - 12 \ln(x/2) & x < 1, \\ 17 + 12 \ln(2) & x \geq 1. \end{cases} \quad (12)$$

Therefore, the emissivity Q assumes the form

$$\frac{dQ}{d\omega}(\omega, z) = \frac{8\alpha}{15} \left(\frac{\alpha}{m} \right)^2 n^2(z, T) \quad (13)$$

$$\times \sqrt{\frac{2T}{m\pi}} \left(1 + \frac{\omega}{T} \right) e^{-\omega/T} h\left(\frac{\omega}{T}\right). \quad (14)$$

To translate this volume emissivity into a spectral surface emissivity we integrate over the positron density distribution given in expression (7). The resulting surface emissivity ($F \equiv \int dz Q(z)$) is defined as the energy emitted per unit time, per unit surface area at a given frequency. The result of integrating expression (10) is,

$$\begin{aligned} \frac{dF}{d\omega}(\omega) &= \frac{dE}{dt dA d\omega} \simeq \frac{1}{2} \int_0^\infty dz \frac{dQ}{d\omega}(\omega, z) \sim \\ &\sim \frac{4}{45} \frac{T^3 \alpha^{5/2}}{\pi} \sqrt[4]{\frac{T}{m}} \left(1 + \frac{\omega}{T} \right) e^{-\omega/T} h\left(\frac{\omega}{T}\right), \end{aligned} \quad (15)$$

where factor $1/2$ accounts for the fact that only the photons emitted away from the core can actually leave the system. Integrating over ω contributes a factor of $T \int dx (1+x) \exp(-x) h(x) \approx 60 T$, giving the total surface emissivity:

$$F_{\text{tot}} = \frac{dE}{dt dA} = \int_0^\infty d\omega \frac{dF}{d\omega}(\omega) \sim \frac{16}{3} \frac{T^4 \alpha^{5/2}}{\pi} \sqrt[4]{\frac{T}{m}}. \quad (16)$$

From equation (15) it is clear that emission from the nuggets will be peaked at frequencies near $\hbar\omega \sim T$ and displays a weak (logarithmic) dependence on frequency when $\hbar\omega \ll T$.

This derivation is identical to that provided in [18] which analyzed thermal emission from nuggets within the galactic centre. That analysis focussed on a possible contribution to the galactic spectrum from the nuggets in the microwave range. As we now want to consider radio band emission it is necessary to treat the low energy tail of the spectrum more carefully.

One may ask how microwave radiation may be emitted from the nuggets when the wavelength λ is much larger than the size of the nugget $\lambda \gg R$. In general this is not a problem—consider the well-known astrophysical emission of the $\lambda = 21$ cm line from hydrogen with a size $a \simeq 10^{-8}$ cm. This example shows that important part of the question is not the size of the system but rather, the coherence time. The coherence time τ of the positrons which must be compared with the formation time $\sim \omega^{-1}$ of the photons. If the coherence time is too short, then multiple scatterings will disrupt the formation of the photons. This suppression is a case of the so-called Landau-Pomeranchuk-Migdal (LPM) effect [28], see also recent application of the LPM effect in similar context of quark dense stars [29].

To estimate the coherence time τ for our case, consider the cross-section σ_{ee} of the positron-positron interaction. This scales as $\sigma_{ee} \sim \alpha^2/q^2$ where $q \sim b^{-1}$ is the typical momentum transfer, and may be expressed in terms of the impact parameter $b \sim n^{-1/3}$, which is estimated in terms of average interparticle spacing where n is the local positron density. The mean-free-path l is thus $l^{-1} \sim \sigma_{ee}n \sim \alpha^2 n^{1/3}$. Therefore, the typical time between collisions (which is the same as coherence time) is $\tau \sim l/v$ where $v \sim \sqrt{T/m}$ is the typical positron velocity.

Collecting all factors together and using (7) for the density profile we arrive at the estimate

$$\omega\tau \sim \frac{\omega}{\alpha^2 n^{1/3}} \sqrt{\frac{m}{T}} \sim \frac{\omega}{\alpha^2 T} \left(1 + \frac{z}{\bar{z}}\right)^{\frac{2}{3}} \geq 1. \quad (17)$$

One can check that this condition is satisfied for $\omega \geq 10^{-4}$ eV and $T \leq 1$ eV even for $z = 0$. Thus, we were marginally justified in omitting LPM effect in our estimates (15) in the low-density regime (7) for $\omega \geq 10^{-4}$ eV, which corresponds to the longest wave length with $\nu \geq 22$ GHz in WMAP haze studies. However, from the same estimate it is clear that this suppression becomes important for smaller frequencies $\omega \ll 10^{-4}$ eV.

We want explicitly take into account the corresponding suppression for radio waves with $\nu \ll 20$ GHz. One can implement this suppression into our formula (15) as follows. First, consider the minimal frequency when condition (17) is marginally satisfied for $z \geq z_{min}$, i.e.

$$\frac{\omega}{T} = \alpha^2 \left(\frac{\bar{z}}{z_{min} + \bar{z}} \right)^{\frac{2}{3}}, \quad \omega_0 = \alpha^2 T. \quad (18)$$

For sufficiently large frequencies $\omega \geq \omega_0$ the LPM effect is not operational anywhere in electrosphere even for $z = 0$. In this case one can integrate over entire region $\int_0^\infty dz$ of

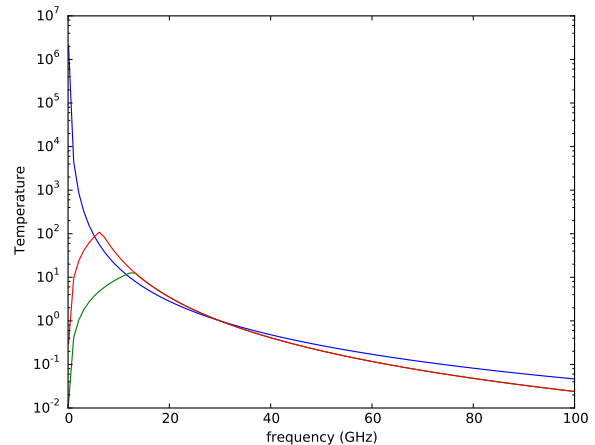


FIG. 1. The spectrum of quark nuggets across the tens of GHz range for nugget temperatures of $T_N = 0.5$ eV (red) and $T_N = 1$ eV (green). Also shown is the power law spectrum reported by Planck with $T \sim \nu^{-2.55}$ continued to the low energy region with the same spectral index. All spectra are normalized at $\nu = 30$ GHz, as such that the total magnitude is arbitrary.

the electrosphere. This is precisely the procedure leading to eq. (15).

However, for radio frequencies $\omega \leq \omega_0$ the LPM effect is operational, at least in some region of z . This effect strongly suppresses the emission of the low energy photons from that region. We want to account for this suppression using the following technical trick. We separate the integral entering (15) into two regions, the high density region, and the low density region correspondingly:

$$\int_0^\infty dz \frac{dQ}{d\omega} = \int_0^{z_{min}} dz \frac{dQ}{d\omega} + \int_{z_{min}}^\infty dz \frac{dQ}{d\omega}. \quad (19)$$

Within the high density region $z \leq z_{min}(\omega)$ the coherence condition (17) is not satisfied and the production of low energy photons is strongly LPM suppressed. Conversely, for $z \geq z_{min}$ the coherence condition is satisfied and photon production proceeds essentially as in vacuum. For our estimate it is sufficient to disregard the emission of the low energy photons from the high density region and focus on emission from $z \geq z_{min}$. In other words, the region of integration in our computation of the spectral surface emissivity (15) becomes frequency dependent,

$$\frac{dF}{d\omega}(\omega) \simeq \frac{1}{2} \int_{z_{min}}^\infty dz \frac{dQ}{d\omega}(\omega, z) \quad \text{for } \omega \leq \omega_0, \quad (20)$$

where z_{min} depends on ω according to (18). Formula (20) is identical to our original formulation (expression 15) for high frequency photons while at low frequencies an ever smaller fraction of the electrosphere contributes to the surface emissivity. The z integration in expression (20) can be easily computed as the density profile has a simple analytical expression as a function of z in the Boltzman

regime (7). The resulting suppression factor $\Delta(\omega) \leq 1$ for $\omega \leq \omega_0$ is convenient to represent as follows:

$$\begin{aligned} \Delta(\omega) &= \left(\frac{\bar{z}}{z_{\min} + \bar{z}} \right)^3 \simeq \left(\frac{\omega}{\alpha^2 T} \right)^{\frac{9}{2}} \\ &\simeq \left(\frac{\omega}{\omega_0} \right)^{\frac{9}{2}} \left(\frac{T_0}{T} \right)^{\frac{9}{2}}, \end{aligned} \quad (21)$$

where $\omega_0 \simeq 10^{-4} \text{eV}$ for $T_0 \simeq 1 \text{eV}$. In deriving (21) we used the fact that the integral entering (20) with density profile (7) leads to the cubic dependence on cutoff as shown in (21). The corresponding density cutoff is further expressed in terms of frequency of emission ω according to (18).

The combination of the spectrum given in equation (15) and the LPM suppression factor of equation (21) allow us to describe the thermal spectrum of the nuggets from the eV scale down to radio frequencies. This spectrum is plotted in Fig.1 showing its similarity to the reported haze spectrum in the tens of GHz range as well as the low energy cutoff.

One should remark here that our treatment of the low frequency part of the spectrum at $\omega \leq \omega_0$ is equivalent to very sharp “removal” of the corresponding emission from the high density region with $z \leq z_{\min}(\omega)$. In Fig.1 this corresponds to almost “cusp” like behaviour of the spectrum. In reality the LPM suppression becomes operational in the extended region of $z \simeq z_{\min}$ with the typical width $\Delta z \simeq \bar{z}$ according to eq. (21). The cusp in Fig.1 will be smoothed out by this modification. However, the basic qualitative behaviour is unaffected by this smoothing and remains the same as plotted in Fig.1. A precise treatment of this transition region where the LPM effect becomes operational is a technically challenging problem. Fortunately, for our purposes we do not need the precise form of this transition region. Therefore, we will use our rough estimates in their present form for the following analysis.

To reiterate: Our procedure employed above obviously introduces some numerical uncertainty of order unity in the suppression factor (21). However, this expression obviously shows that the radio wave emission is strongly suppressed by this mechanism, while emission at CMB frequencies with $\omega \geq \omega_0$ remain essentially untouched by this suppression.

C. Other potential correction factors in radio emission bands

The previous subsection analyzed the key factor, the LPM suppression which influences the radio emission from dark matter nuggets, which is the main subject of the present studies. We now want to consider some other sources which may also affect the low energy radio emission.

1. The mean-field approximation which we explored in deriving expression (7) is not valid for extremely

large z , where exponential rather than power-law decay is expected. We could accommodate the corresponding feature by introducing a cutoff at some sufficiently large $z = z_{\max}$ on the order the radius of the nugget $R \sim 10^{-5} \text{cm}$. The result, however, is not sensitive to this cutoff, so we use $z_{\max} = \infty$ in our formula (15). This cutoff at very large $z = z_{\max}$ does not affect our expression for the suppression factor (21) because at large z_{\max} the positron density is already small enough to contribute little to the overall emissivity.

2. Our calculations have assumed that we are working in infinite matter. However, the nuggets have a finite extent on the order of $R \geq 10^{-5} \text{cm}$. In principle, finite-size effects may change the positron scattering cross-section (9), and therefore, our estimation of the emissivity (10). The cross-section (9) was derived using a continuum of plane-wave states, whereas to account for the finite-size effects, one should use the basis of states bound to the quark core. To estimate the size of the corrections, one can imagine confining the positrons to a box of finite extent R . The electromagnetic field may still be quantized as in free-space with states of arbitrarily large size because the photons are not bound to the core, and are not in thermodynamic equilibrium with the positrons. Their mean-free-path is much larger than R , so the low-energy photons produced by the mechanism described above will simply leave the system before they have a chance to interact with other positrons.

Therefore, it is only the positron states that must be considered over a finite-size basis, which will modify the corresponding Green’s function used in the calculation of the cross-section (9). These modifications occur for momenta of the scale $\delta p \sim \frac{n\hbar}{R}$ with n being an integer number describing the typical excitation level. If $R \geq 10^{-5} \text{cm}$, then this corresponds to shifts in the energies of $\delta E \sim (\delta p)^2/2m \sim 10^{-6} \text{eV} \ll 10^{-4} \text{eV}$, which is much smaller than the transitions responsible for the emission at microwave frequencies. One could naively think that this energy shift could affect emission at radio frequencies $\omega \sim 10^{-6} \text{eV}$, which is the main subject of the present work. However, this is not the case because the typical positron energy scale is determined by the nugget temperature $T_n \sim 1 \text{eV}$ corresponding to very large excitation numbers $n \gg 1$ for the positrons responsible for emission. Thus, we conclude that finite-size effects do not drastically change the positron Green’s function in the region of interests. In other-words, the expression for the cross-section (9)—derived using the standard (infinite volume) Green’s functions—remains valid for our estimation of the emission and spectrum down to radio frequencies when $T_n \sim 1 \text{eV}$, and we may use our original expressions for the emissivity (13) and suppression (19), (21). We also note that finite-size effects do not change our estimates for the density (6) because the finite-size effects $\delta E \ll T$ are much smaller than the typical energetic scale $T_n \sim \text{eV}$ of the problem. Thus, our expression (9), and therefore (15) remains valid even for radio frequency photons which is the main subject of the present

studies.

3. Another factor which may potentially affect the low energy emission from the nuggets is the generation of the plasma frequency $\omega_p^2 = \frac{4\pi\alpha n}{m}$ in the electrosphere. The plasma frequency can be thought as an effective mass for the photon: only photons with energy larger than this mass can propagate within the system and eventually escape the nugget. Photons with $\omega < \omega_p$ are “off-shell” or “virtual”: these can only propagate for a short period of time/distance $\sim \omega_p^{-1}$ before they decay (are absorbed). This effect, similar to the LPM effect, also suppress the low energy emission. However, the physics of generating the plasma frequency are different from those involved in the LPM effect discussed in the previous section IV B. The observable manifestations of this phenomenon are also different from the LPM effect –the low energy photons, even if they are produced, can not propagate in an environment with non vanishing ω_p . This should be contrasted with LPM effect in which low energy photons cannot be even formed.

One can estimate that the plasma frequency ω_p is in the few eV range for densities (7) at $z = 0$ and even smaller for large $z > 0$. Given our previous discussion, one might ask: How can low-energy photons $\omega < \omega_p$ which are the subject of the present work, still be emitted? The reason is that, although these photons would be reabsorbed in infinite matter, this reabsorption happens on a length scale of ω_p^{-1} . At the typical densities in the Boltzmann regime, $\omega_p^{-1} \sim 0.3 \cdot 10^{-5}$ cm is much larger than $\bar{z} \sim 10^{-8}$ cm where such high density is supported by the nugget’s structure (8). Therefore, many of these photons will have left the nugget before being reabsorbed. Therefore, this effect is important in the deep dense regions of the nuggets. It would be also important if our system would be infinitely large. However, the generating of the plasma frequency ω_p does not affect our expression for the emissivity (13) and corresponding estimates (19), (21) for finite size nuggets the in radio bands, which is the subject of our present studies.

To conclude this section: with the estimates just presented we are now in position to consider the potential for radio band observations to search for the presence of quark nugget populations within our own or nearby galaxies.

V. RADIO BAND INTENSITY CALCULATIONS

The emission spectrum of a quark nugget within a given environment is determined by its temperature. In the case of an antiquark nugget the primary heating mechanism is the annihilation of visible matter within the nugget². Within the galactic interstellar medium (ISM)

the flux of matter onto the nuggets is simply the product of the local visible matter density and the mean velocity. The total heating rate of the nugget is then given by,

$$\frac{dE}{dt} = \rho_{\text{vis}} v f_T \sigma_N \quad (22)$$

where f_T is the fraction of colliding mass which annihilates and thermalizes within the nugget and σ_N is the nugget cross-section. Equating this heating rate with the rate of thermal emission from equation (16) gives the nuggets’ radiating temperature in a given environment:

$$T_N = 0.5 \text{ eV} \left[\frac{\rho_{\text{vis}}}{10 \text{ GeV/cm}^3} \frac{v}{200 \text{ km/s}} f_T \right]^{4/17}. \quad (23)$$

This temperature fixes the emission spectrum of an individual nugget. Using eqs.(15) and (16) the corresponding spectrum can be written in the following form,

$$\frac{dE}{dt d\omega} = \frac{\rho_{\text{vis}} v \sigma_N f_T}{60T} \left(1 + \frac{\hbar\omega}{T} \right) e^{-\hbar\omega/T} h \left(\frac{\hbar\omega}{T} \right). \quad (24)$$

The volume emissivity of the ISM due to the presence of quark nugget dark matter is then given by scaling the individual nugget spectrum by the number density of nuggets,

$$\begin{aligned} \epsilon_N &\equiv \frac{dE}{d\omega dt dV} = \frac{\rho_{DM}}{M_N} \frac{dE}{d\omega dt} \\ &= \frac{\rho_{\text{vis}} v \sigma_N \rho_{DM} f_T}{90 M_N T} \left(1 + \frac{\hbar\omega}{T} \right) e^{-\hbar\omega/T} h \left(\frac{\hbar\omega}{T} \right) \end{aligned} \quad (25)$$

where M_N is the average quark nugget mass and we have included a factor of 2/3 to account for the fact that only the antiquark nugget component of the dark matter will contribute to the radio band spectrum. As established in the low frequency treatment of section IV B expression (25) must be multiplied by the suppression factor (21) for frequencies below $\omega \sim \alpha^2 T$.

Note that the physical properties of the nuggets entering into expression (25) are carried by the cross section to mass ratio σ_N/M_N . There is also a dependence on the thermalization coefficient f_T both as an overall scaling factor and through the dependence of emissivity on the radiating temperature (from equation 23) however the value of f_T is expected to fall in the range $1 > f_T > 1/2$ so this factor contributes only marginally when compared to the much larger allowed range of σ_N/M_N . Note that $\sigma_N \sim B^{2/3}$ while $M_N \sim B$ so that the cross section to mass ratio scales with the nugget baryon number as $B^{-1/3}$. As already mentioned in the Introduction this small geometrical factor replaces the weakness of the visible-dark matter interaction in conventional WIMP paradigm.

² Nuggets composed of quarks rather than antiquarks will experience purely collisional heating and will be at a much lower

temperature. Consequently we may safely neglect their impact on the galactic spectrum.

A. Matter distributions

The emissivity given in equation (25) allows us to determine the thermal emission from a population of quark nuggets provided we know the distribution of matter and dark matter. We will adopt the standard Navarro-Frenk-White (NFW) profile,

$$\rho_{NFW}(r) = \rho_s \left(\frac{r_s}{r} \right) \left(1 + \frac{r}{r_s} \right)^{-2} \quad (26)$$

so that the dark matter profile of a given galaxy may be described by the scale radius (r_s) and the characteristic density (ρ_s). For example the dark matter halo of the Milky Way is generally taken to have $r_s \approx 22$ kpc and $\rho_s \approx 0.5 \text{ GeV/cm}^3$. The visible matter distribution is generally more complicated and, for present purposes, we will attempt to capture only its basic properties. Of primary importance in the context of dark matter interactions is the central, spherically symmetric, galactic bulge. We will model the bulge with a simple exponential,

$$\rho_B(r) = \rho_0 e^{-r/r_0} \quad (27)$$

with central density ρ_0 and scale length r_0 . For a Milky Way like galaxy we expect $r_0 \approx 3 \text{ kpc}$ and $\rho_0 \approx 100 \text{ GeV/cm}^3$. Additionally we will include a disk component for the visible matter,

$$\rho_d(h) = \rho_d e^{-h/H_0} \quad (28)$$

where h is the height above the galactic plane, ρ_d is the in plane density and H_0 is the disk scale height. For a Milky Way like spiral we may estimate the central disk density as $\rho_d \approx 1 \text{ GeV/cm}^3$ and a disk scale height of $H_0 \approx 0.5 \text{ kpc}$. The disk distribution will be cut off at a maximum distance d_{max} from the galactic centre.

The final property of the galactic matter distribution we need is the average velocity. While some galactic matter has been significantly accelerated the majority carries a velocity on the order of the galactic rotation speed. As such we will consider the average velocity of the matter populations to be on the order of $v \sim 200 \text{ km/s}$.

B. Milky Way

The flux received from the quark nugget population within our galaxy may be determined by the integral of the emissivity given in expression (25) along a given line of sight. We are particularly interested in the intensity received from the direction of the galactic centre where both the dark and visible matter distributions are strongly peaked. For simplicity we here consider ignore the visible matter in the disk and focus on the bulge component which strongly dominates along lines of sight through the galactic centre. This introduces a rotational

symmetry and somewhat simplifies the integration procedure. In this case the flux received from a line of sight through the galactic centre is given by

$$\Phi = \int \frac{dV}{4\pi r_\odot^2} \epsilon(r_g), \quad (29)$$

where r_\odot is the distance from earth and r_g is total distance from the galactic centre. Exploiting the rotational symmetry of the problem this may be simplified to give

$$\Phi = \int_0^\infty dr \int_0^{h_{max}} \frac{h dh}{h^2 + r^2} \epsilon(r_g) \quad (30)$$

where r is radial distance from earth along the galactic plane and h is height above the plane. Thus $r_g \equiv \sqrt{(R_\odot - r)^2 + h^2}$ where R_\odot is the earth's distance from the galactic centre. The maximum height (h_{max}) appearing in equation (30) is determined by the solid angle observed with $h_{max} = r \tan \phi$ where ϕ is the angular resolution of the observation. Performing the integration in equation (30) with an assumed $\sim 10'$ resolution to match the Planck data produces the spectrum shown in figure (2). As can be seen in that plot nuggets with a baryon number of $B \approx 10^{25}$ would saturate the observed haze signal from the inner galaxy. This establishes a lower limit on the nugget size based on the Planck data. Note that the LPM cutoff discussed in section IV B does not play a role at the frequencies observed by Planck, though can it is shown at low frequencies in figure 2.

It should be made clear that quark nugget dark matter, while it can reproduce the spectrum shown in Fig. 2 with $B \sim 10^{25}$ nevertheless cannot explain all the other observed features of the haze and, as such, producing the full observed flux observed at the galactic centre represents an upper limit of the nugget contribution. Thermal emission from the nuggets necessarily tracks the matter density and cannot explain the haze emission at large galactic latitudes, the quark nugget spectrum will also fail to produce a hard edge to the haze emission as is observed at large latitudes. Furthermore the emission from the nuggets will be completely unpolarized, so the polarized component observed to trace the edges of the haze emission must be produced by other astrophysical mechanisms. Our proposal here is that emission from the quark nuggets will provide additional contribution to the total haze emission at low latitudes and, from this picture, to extract limits on the allowed parameter space of quark nugget dark matter.

C. Nearby Milky Way like galaxies

Finally we turn to emission from nearby spiral galaxies with matter distributions believed to be similar to that of our own galaxy. In this case we will determine the total radio band emission from a galaxy. This is done by integrating emissivity (equation 25) including the suppression factor (21) over the entire matter distribution (this

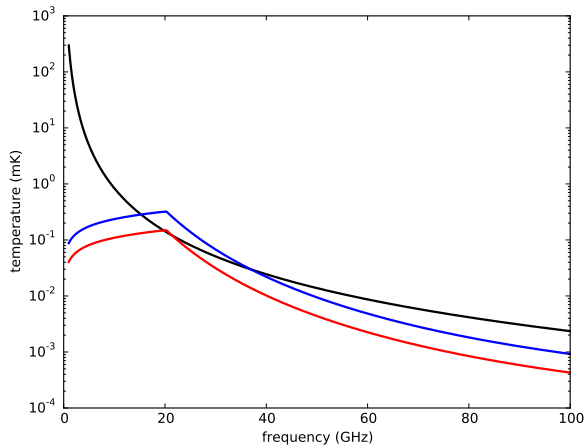


FIG. 2. The spectrum of quark nuggets across the tens of GHz frequencies observed by WMAP and Planck. The haze spectrum as reported by Planck is plotted in black, continued to the low energy region with the same spectral index $T \sim \nu^{-2.55}$. The spectra for a quark nugget population with $B \sim 10^{25}$ is plotted in blue and that of a population with $B \sim 10^{26}$ is shown in red. The nugget contribution that from the $B \sim 10^{25}$ population would saturate the haze emission from the galactic centre and, as such, any mean baryon number below this value is effectively ruled out by the current Planck data. See text for more specific discussion of limits.

time including the disk contribution which may be significant in this case as an extended faint disk can make a relatively large contribution to total emission.) Once we have established the total emission from a spiral galaxy the flux as observed on earth may be obtained from the inverse square law. Thus,

$$\Phi = \frac{1}{4\pi d^2} \int d^3r \epsilon(r) \quad (31)$$

where, d is the distance to the galaxy. Taking the lower bound obtained from the Milky Way observations discussed in section VB we may extrapolate the observational consequences for nearby Milky Way like galaxies. For simplicity consider a test galaxy with physical parameters identical to those used in our discussion of the Milky Way in section VB. We may then translate the total intensity in the radio band to a simple distance flux relationship. The results of this process, assuming a mean nugget size of $B \sim 10^{25}$ which would saturate the galactic haze, are shown in Fig.3. As can be seen the strong suppression of radio band emission results in a galactic radio signal below the observed level in all cases.

This result is in drastic contrast with the studies of [1] which claimed that radio observations of nearby spiral galaxies essentially rule out any significant dark matter contribution to the galactic haze. The difference of course results from our specific dark matter model in which radio emission is strongly suppressed while the emission at CMB frequencies is unaffected by the suppression ef-

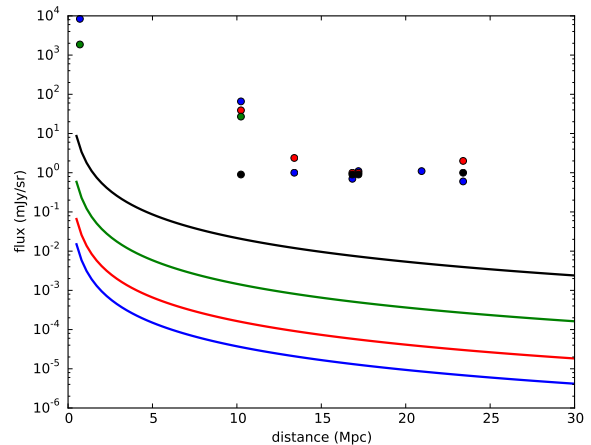


FIG. 3. Intensity predictions for the quark nugget population of a nearby Milky Way like galaxy as a function of distance for a variety of wavelengths. Note that the totally emission at a given distance is strongly suppressed in the radio bands due to the LPM effect as discussed in the text. Also shown are a variety of radio observations as used in [1] to constrain a conventional dark matter contribution to the galactic haze. Shown are the predicted nugget flux (solid lines) and the observed radio signals from nearby galaxies as reported in [1] (dots) the colours indicate frequency with 1.49GHz in blue, 2.38GHz in red, 4.85GHz in green and 15GHz in black.

fects studied in sections IV B and IV C. The constraints derived in [1], remain fully valid for WIMP type dark matter models which are not subject to these suppression mechanisms and predict a smooth extrapolation between microwave and radio frequencies.

VI. CONCLUSIONS

It has been demonstrated here that astronomical observation at radio frequencies provide only weak constraints on quark nugget dark matter. The fundamental reason for this is that thermal emission from the nuggets is suppressed at low energies by many body effects within the outer layers of the nuggets. This effect is specific to compact composite dark matter models and will not be seen in more conventional dark matter models which argue for a haze produced by the relativistic products of dark matter annihilations or decays. Consequently the strong constraints derived in [1] are entirely valid for WIMP type dark matter models and the suppression effect which we discuss here is relevant only in the case of quark nugget dark matter.

One should note here that in previous studies we did discuss isotropic radio emission in the GHz band due to the same quark nugget model [21]. Furthermore, we claimed in [21] that the excess in the isotropic radio background at frequencies below the GHz scale measured by the ARCADE 2 experiment can be naturally explained

by the same dark matter model studied in the present work. The difference between our present analysis in the radio band and our previous study is that the emission analyzed in [21] originated at higher (unsuppressed) frequencies but at very earlier times with $z \sim 10^3$ and has subsequently redshifted into the radio, this work deals exclusively with the present epoch and (strongly suppressed) radio emission originating in the GHz band.

Across most of the observable parameter space low energy suppression comes into effect below the 10-20GHz range. As such the most useful channels for investigating quark nugget dark matter are above this scale. For example, improved Planck observations of the Andromeda galaxy [30] may be able to examine a possible haze component from the bulge of Andromeda. Ground based radio and microwave observations around 20GHz may also be capable of constraining the possible nugget contribution to the spectrum of nearby galaxies, however these constraints will be dependent on the exact details of the low energy LPM cutoff.

In conclusion the dark matter proposal advocated in this work may explain a number of apparently unrelated

puzzles as reviewed in section III B. All these puzzles independently suggest the presence of some source of excess diffuse radiation in different bands ranging over 13 orders of magnitude in frequency. The new element highlighted in this paper is that the same DM model is not strongly constrained (and certainly, not ruled out) by the analysis [1]. This is in contrast with vast majority of conventional WIMP's models in which the low energy spectrum continues from microwave frequencies to radio frequencies with similar spectral index and whose contribution to the haze signal is strongly constrained by [1].

ACKNOWLEDGEMENTS

We are tankful to Ludo Van Waerbeke who brought our attention to analysis [1], which eventually initiated these studies. We are also thankful to him for discussions, questions and comments. This research was supported in part by the Natural Sciences and Engineering Research Council of Canada.

-
- [1] E. Carlson, D. Hooper, T. Linden and S. Profumo, JCAP **1307**, 026 (2013) [arXiv:1212.5747 [astro-ph.CO]].
 - [2] D. P. Finkbeiner, Astrophys. J. **614**, 186 (2004) [astro-ph/0311547].
 - [3] Planck Collaboration, AAP **554**, A139 (2013).
 - [4] E. Witten Phys.Rev. D **30**, 272 (1984).
 - [5] G. Dobler *et al.*, Astrophys. J. **717**, 825-842 (2010).
 - [6] M. Su, T. R. Slatyer and D. P. Finkbeiner, Astrophys. J. **724**, 1044-1082 (2010).
 - [7] Planck Collaboration, *preprint* arxiv:1506.06660 (2015).
 - [8] G. Dobler, APJ **750**, 17 (2012).
 - [9] A. E. Egorov, J. M. Gaskins, E. Pierpaoli and D. Pietrobon, arXiv:1509.05135 [astro-ph.CO].
 - [10] A. R. Zhitnitsky, JCAP **0310**, 010 (2003) [hep-ph/0202161].
 - [11] D. H. Oaknin and A. Zhitnitsky, Phys. Rev. D **71**, 023519 (2005) [hep-ph/0309086].
 - [12] A. Zhitnitsky, Phys. Rev. D **74**, 043515 (2006) [astro-ph/0603064].
 - [13] K. Lawson and A. R. Zhitnitsky, Cosmic Frontier Workshop: Snowmass 2013 Menlo Park, USA, March 6-8, 2013. [arXiv:1305.6318].
 - [14] M. G. Alford, A. Schmitt, K. Rajagopal and T. Schäfer, Rev. Mod. Phys. **80**, 1455 (2008) [arXiv:0709.4635 [hep-ph]]
K. Rajagopal and F. Wilczek, The Condensed Matter Physics of QCD, (2000) [arXiv:hep-ph/0011333]
 - [15] D. H. Oaknin and A. R. Zhitnitsky, Phys. Rev. Lett. **94**, 101301 (2005), [arXiv:hep-ph/0406146].
 - [16] A. Zhitnitsky, Phys. Rev. D **76**, 103518 (2007), [arXiv:astro-ph/0607361].
 - [17] K. Lawson and A. R. Zhitnitsky, JCAP **0801**, 022 (2008), [arXiv:0704.3064 [astro-ph]].
 - [18] M. M. Forbes and A. R. Zhitnitsky, Phys. Rev. D **78**, 083505 (2008) [arXiv:0802.3830 [astro-ph]].
 - [19] M. M. Forbes, K. Lawson and A. R. Zhitnitsky, Phys. Rev. D **82**, 083510 (2010). [arXiv:0910.4541 [astro-ph.GA]].
 - [20] M. M. Forbes and A. R. Zhitnitsky, JCAP **0801**, 023 (2008) [astro-ph/0611506].
 - [21] K. Lawson and A. R. Zhitnitsky, Phys. Lett. B **724**, 17 (2013) [arXiv:1210.2400 [astro-ph.CO]].
 - [22] IceCube Collaboration, Eyr. Phys. J. C **74**, 2938 (2014).
 - [23] P. W. Gorham, Phys. Rev. D **86**, 123005 (2012), [arXiv:1208.3697 [astro-ph.CO]].
 - [24] K. Lawson, Phys. Rev. D **88**, 043519 (2013), [arXiv:1208.0042 [astro-ph.HE]].
 - [25] A. W. Strong, I. V. Moskalenko and O. Reimer Astrophys. J. **613**, 962-976 (2004).
 - [26] M. P. Muno *et al.*, Astrophys. J. **613**, 326 (2004) [astro-ph/0402087].
 - [27] P. W. Gorham and B. J. Rotter, arXiv:1507.03545 [astro-ph.CO].
 - [28] L. D. Landau, and I. Pomeranchuk, Dokl. Akad. Nauk. Ser. Fiz. **92**, 535 (1953);
A. B. Migdal, Dokl. Akad. Nauk. S. S. S. R. **105**, 77 (1955).
 - [29] P. Jaikumar, C. Gale, D. Page and M. Prakash, Phys. Rev. D **70**, 023004 (2004) [astro-ph/0403427].
 - [30] Planck Collaboration, [arxiv:1407.5452] (2014).